



Numerical modeling for episodic thermal convection in Enceladus ice shell

This Dissertation is Submitted for the Degree of
Geoscientist

Mariana Carolina Villamil Sastre

Universidad de los Andes
Faculty of Science
Geosciences Department

Bogotá D.C. Colombia
2018



Numerical modeling for episodic thermal convection in Enceladus ice shell

This Dissertation is Submitted for the Degree of

Geoscientist

Mariana Carolina Villamil Sastre

Universidad de los Andes
Faculty of Science
Geosciences Department

Advisor
Jillian Pearse. Ph.D

Bogotá D.C. Colombia
2018

*To my grandma Sara and her promise to live long enough to see
me working at NASA*

Acknowledgements

First and foremost, I want to thank my family, my mother Nancy and my sister Angelica, for supporting me in every moment of my life and giving me the strength to keep going despite the adversities. To my grandmother Sara, for keeping me in her few memories. All of you are part of who I am and are the reason why I strive every day to get at NASA.

Second, I should like to thank my supervisor Dr. Jillian Pearse, for supporting me in the development of this degree project and for believing in my skills and passion in planetary sciences. Also, for the knowledge that I got as her student and teaching assistant.

On the other hand, I want to thank Dr. Alejandro Garcia for his unconditional support during these years of research work. Thank you to believe in me and to open the doors to astronomy and guide me to the study of the solar system. Also, I must thank Dr. Juan Pablo Mallarino for helping me in the handling of the cluster and parallel computing, his collaboration was crucial in this degree work.

I must thank my colleagues and friends, especially to Diana Lozano for join me in the most difficult moments during the course of my two careers. Thanks to David Paipa, for his unconditional presence in this last semester, to Javier Acevedo for helping me to solve the innumerable problems that were presented to me at a technical level and for reminding me that there is always a way out and Juan Pablo Galán for helping me with the corrections. Finally, I want to thank Fabio Pablo Méndez, the best friend that life could give me.

Numerical modeling for episodic thermal convection in Enceladus ice shell

Mariana Carolina Villamil Sastre

Universidad de los Andes

Abstract

In this research we investigate how Enceladus, one of Saturn's most important moons maintains the heat observed by Cassini spacecraft. The existence of an episodic thermal convection in the Enceladus crust is proposed, with numerical models of finite elements in spherical coordinates, which include geodynamical parameters such as tidal forces, a non-uniform viscosity in the crust and a type of convection under a layer not convective. In addition, it is included in the model that the convection is taking place episodically, giving rise to events of maximum heat transport in a span of a few million years and a consequent stability, allowing that the high heat flow can be explained as the release of heat stored in the past. The model is designed to obtain an energy value close to the data obtained by the Cassini mission.

Modelación numérica para convección termal episódica en la corteza helada de Encelado

Mariana Carolina Villamil Sastre

Universidad de los Andes

Abstract

En este trabajo de grado, se busca investigar cómo Encelado uno de los satélites más importantes de Saturno, mantiene el calor observado por los instrumentos de medición de la sonda Cassini en sus primeros sobrevuelos en el año 2005. Se propone la existencia de una convección termal episódica en la corteza de Encelado, con modelos numéricos que incluyen el método de elementos finitos en coordenadas esféricas con parámetros geodinámicos tales como las fuerzas de marea, viscosidad no uniforme en la corteza y un tipo de convección bajo una capa no convectiva. Además, se incluye en el modelo que la convección se lleva a cabo de forma episódica, lo que da lugar a eventos de transporte máximo de calor en un lapso de millones de años y una estabilidad consecuente. Permitiendo que el alto flujo de calor se pueda explicar como la liberación de calor almacenado en el pasado. El modelo está diseñado para obtener un valor de flujo de energía cercano a los datos obtenidos por la misión Cassini.

Contents

1	Objectives	3
1.1	General Objective	3
1.2	Specific Objectives	3
2	Introduction	4
3	Simulations Models	7
3.1	Equations	7
3.2	Finite-element code	8
3.3	CitcomS	9
3.4	Models Description	10
4	Input files	11
4.1	Parameters	11
5	2D-Convection Model	13
5.1	Theory	13
5.1.1	Rayleigh number	13
5.1.2	Prandtl number	14
5.1.3	Reynolds number	14
5.2	Method	14
5.2.1	Time-evolution simulation	15
5.3	Results	16
6	3D-Convection Model	18
6.1	Method	18
6.1.1	Running simulations in the cluster	18
6.1.2	MPI computing	19
6.1.3	HDF5 files	20
6.2	Results	21
6.2.1	0 Million years	21
6.2.2	50 Million years	21
6.2.3	100 My	22
7	Conclusions	25

Chapter 1

Objectives

1.1 General Objective

To model numerically the Enceladus ice shell in an episodic thermal convection, which is not geometrically uniform and compositionally differentiated.

1.2 Specific Objectives

- To create a computational model of finite elements in spherical coordinates for the flow of heat in an incompressible material.
- To interpret the data obtained by the Cassini mission, in order to parameterize the numerical model.
- To establish a period of time with the ability to sustain the model and show the values obtained by Cassini.

Chapter 2

Introduction

In 2005, Cassini mission made a historical finding: within the trajectory of its orbit was found geothermal activity in Enceladus south pole. Enceladus is one of Saturn's moons whose orbit is between Mimas and Tethys. In that zone, there are Y-shape fractures, whose terrain is geologically younger than the rest of the surface. These fractures are called the “Tiger Stripes”, and are defined as linear depressions with a depth close to 500 m and 2 Km wide and 130 Km long, which usually in the southern hemisphere are bifurcating in dendritic patterns. This area is 10 percent brighter than the rest[2].

Besides, geomorphologically, the south pole is made up of ridges and valleys where it is possible to find the deposits resulting from the fractures. The brightness on the Enceladus surface can be the result of the presence of a thin layer that covers it with regolith [2]. That material is coming from Saturn's E ring by crushing the particles. The stripes in some locations are deflected to form quasi-circular patterns that can represent relaxation[9] and degradation of the impact craters, or analyzed from the geomorphology, can be the evidence of diapirs in the subsoil.

Longitudinally, the orogeny average is 400 m below the reference ellipsoid (theoretical form), and latitudinally at 45 S is 400 above it [2]. If Enceladus were homogeneous internally, its shape would be close to the equilibrium ellipsoid (hydrostatic shape controlled by gravity and precession)[4], and it would also support between 250 and 500m of topography relative to the geoid (equipotential surface of the planetary body).

The geysers' geometry determines the particle expulsion angle and what fraction of these particles is given in micrometers. Assuming a regional ocean, it must be fulfilled that the heat is enough to raise the temperatures to 273 K for a very localized event near to the surface, either by tidal friction or precession[3]. In that way, Enceladus was thought as a body being globally heterogeneous with some colder regions, where the south pole could currently be the only place with a localized ocean. However, in this model, a completely different Enceladus is redesigned.

The material that emerges from these fractures has been studied by spectroscopy, being consistent with a composition of pure water, ice grains of the order of micrometers, and organic material.[2] This moon is geologically distinguished and its surface is the most reflective in the solar system. The geological activity shows an age of approximately 4 billion years and the areas of the South Pole date from 500,000 years or even less.

Cassini’s scientific team (Porco, et. al) attribute this geological activity as the result of the tidal forces on Enceladus when it enters into resonance with other satellites, establishing in the past a variable eccentricity and unstable orbit that allowed the generation of observed heat (4-7GW) [10]. On the other hand, some investigations show the heat flow as a product of the shear friction observed in the Tiger Stripes; this allows the sublimation of an underground ocean in the south pole of Enceladus [3].

Enceladus can also be wrapped in a 2:1 resonance with Janus, the last one is only 1000 km away from the resonance, but in the past could have been in that configuration [4]. If Janus were in resonance when the eccentricity of Enceladus was low, the probability of capture in the resonance of Enceladus would have been high, so if these satellites were in an equilibrium configuration, models ensure that 4.5 GW of heat would be observed, which is consistent with the first observations [11]. The resonance with Janus can explain the surface renewal events but would have to attend to a meteorite impact to get the actual resonance system. An alternative is that Janus became unstable when Enceladus reached the resonance with Dione. Also, Enceladus is currently forced into a resonance 2:1. It means that for every two revolutions completed by Enceladus, Dione completes one revolution. The ages were calculated in the first investigations in two scenarios: Taking into account the geochronology of lunar impacts with radioactive decay and with a constant flow model of impact craters [21].

Some thermodynamic models explain the dynamics of the fractures by the grain size of the salient particles. An average velocity of the particles of 60 m/s has been calculated, which is much lower than the escape velocity (235 m/s). This situation implies a renewal of the surface by the grains that fall back. In these models, it is shown that only 1 % of particles that came out from the geysers manage to escape and take place into the Saturns E ring [3].

Any mechanism for supplying energy must pass the “Mimas Test”, it means that any theory that claims to explain the observed heat flux in Enceladus must also explain the entirely frozen water of Mimas. This satellite has an ancient surface, it is closer to Saturn than Enceladus and has a greater orbital eccentricity. In such a way, any model of tidal heat carried out in Enceladus must agree with the observed behavior of Mimas[7], this satellite has a surface with a large number of impact craters, which implies that Mimas does not have active tectonics.

In general, there is always research with a physics approach in which the solution to the heat observed in Enceladus is proposed with torques and energy-momentum conservation, without taking into account the rheological characteristics of the satellite. On the other hand, there is a geological approach where heat is solved with tools of structural geology and petrology, excluding the fundamental forces that involve the system. It is possible to find investigations where both approaches converge and are more accurate and realistic with the values observed by Cassini.

In the 43rd Lunar and Planetary Science Conference, the work named: “The impact of a weak south pole on thermal convection in Enceladus’ ice shell” was presented, where its authors Han, L., Tobie, G., Showman, AP (2012) propose the existence of thermal convection in Enceladu’s crust, with numerical 3D models that they include tidal heating and the basal heating. In these models, it is assumed the boundary conditions where there are no asymmetries between the north and the south pole, but given the active tectonism observed in the south pole, it may contain a

weak lithosphere. This part of the crust is characterized by a lower viscosity contrast concerning the north pole (almost three orders of magnitude). In that way, there would be developing "stagnant-lid convection", which describes a convection below of a non-convective layer, showing a significant difference between the north and the south. Having a weak south pole, the models show the presence of plumes reaching the surface, as observed by Cassini. The heat flow obtained in that research was approximately 3-5GW. Still, the revised value with remote sensing detectors for this flow is about 16 GW, of which 0.32 GW comes from radiogenic heat, and the estimated tidal heat is 0.12 GW. As an open conclusion, the authors propose that the convection is taking place episodically, allowing occasional peaks in the heat transport and the currently observed heat flux could be explained as an unusual event in a heat flow system in a shorter time.

To understand how convection occurs in Enceladus, L. Han research work [1] suggest modeling the satellite as an undifferentiated body and with 100 km crust thickness. When stagnant-lid convection is proposed in the north pole, it is assumed that the thermal gradient is limited in this area and free in the south pole [6]. If there were a compositional difference, it could be said that convection is given by differentiation, but the data of the presence of ammonia are not enough to prove it. However, a viscosity contrast is taken between the north and south poles, the latter being the less viscous.

Chapter 3

Simulations Models

3.1 Equations

For modeling the thermal convection in Enceladus crust, taking into account the basal heating and the tidal heating, it is necessary to study fluid mechanics equations, where the behavior of each infinitesimal element will be modeled in spherical geometry. Initially, a finite number of Prandtl is assumed —dimensionless number proportional to the quotient between moment diffusivity (viscosity) and thermal diffusivity. Besides, in [1] the authors make a Boussinesq approximation for incompressible material: This approach is applied to problems where the fluid density varies concerning the temperature from one place to another, driving a fluid flow and heat transfer, complies with the conservation of mass, momentum, and energy. Following [14], if u is the local velocity of a fluid package, the continuity equation for the conservation of the mass is:

$$\boxed{\frac{\partial \rho}{\partial t} + \nabla \cdot (\rho u) = 0}$$

For thermal convection, the density variations associated with thermal expansion are small, for that reason these variations tend to be 0:

$$\nabla \cdot (\bar{\rho} u) = 0$$

Where $\bar{\rho}$ is a reference density that depends on depth

$$\boxed{\nabla \cdot u = 0}$$

Now the general expression for the conservation of momentum for an incompressible fluid (Navier-Stokes equations):

$$\frac{\partial u}{\partial t} + u \cdot \nabla u = \frac{-1}{\rho} \nabla p + \nu \nabla^2 u + \frac{1}{\rho} F$$

Where ν is the kinematic viscosity and F is the sum of any force on the body as well as gravity. In this equation, it is assumed that density variations have a fixed part and another that has a linear dependence on temperature:

$$\rho = \rho_0 - \alpha \rho_0 \Delta T$$

Where α is the coefficient of thermal expansion. If $F = \rho g$ is the gravitational force in a body, we have that the conservation equation becomes:

$$\frac{\partial u}{\partial t} + u \cdot \nabla u = \frac{-1}{\rho} \nabla p + \nu \nabla^2 u + \frac{1}{\rho} g \alpha \Delta T$$

In the heat flux equation in a temperature gradient, the heat capacity per unit volume, C , is supposed to be constant. The resulting equation is:

$$\boxed{\frac{\partial T}{\partial t} + u \cdot \nabla T = k \nabla^2 T + \frac{J}{\rho C_\rho}}$$

Where J is the rate per unit volume of internal heat production and κ is the thermal diffusivity.

In general, we have presented the formality of the equations that governs this type of problem in fluid mechanics, rewriting these equations for the problem we wish to solve in Enceladus:

$$\frac{\partial \sigma_{ij}}{\partial X_j} + R_a T \hat{j} = 0$$

$$\frac{\partial u_i}{\partial X_i} = 0$$

$$\frac{\partial T}{\partial t} + u_i \frac{\partial T}{\partial X_i} = \frac{\partial^2 T}{\partial X_i^2} + A$$

Where σ_{ij} is the stress tensor, T is temperature in Kelvins, A is the tidal heating rate, \hat{j} is the unitary vector in y direction, t is time in Ma, X_{ij} are the spatial coordinates and R_a is the Rayleigh number [1].

This last parameter refers to a dimensionless number that provides information on how heat is transferred inside a material. When the Rayleigh number is below a critical value, heat transfer occurs mainly by conduction. On the other hand, when it is above significant value, heat transfer occurs by convection. This number is going to be variable along with the all research, for modeling and facility reasons.

3.2 Finite-element code

This method is a computational tool to solve some partial differential equations (PDE) used in science for a lot of variational problems. The technique uses an integral of the differential equation over the domain that the user is working. This domain is divided into finite elements, a polynomial function approximates the partial solution of the PDE on each "sub-domain" and the final solution involves the sum of all integrals that contributes to the entire domain. This discretization is equal to partition the problem domain into nodes and elements. It is necessary to define which formulation is going to be used (Lagrangian or Eulerian) because each one has a different way to explain the motion of the particles in a fluid.

For this research, we use CitcomS, which uses a Lagrangian formulation, to improve the convergence for significant viscosity variations. This is a finite-element code capable of solving the equations in 3D, using a longitude-latitude grid, and dividing the sphere into 12 domains; each one is already sub-divided into another grid (with a size equal to 1.5 longitude-latitude).

3.3 CitcomS

CitcomS (California Institute of Technology Convection in the Mantle) was originally written in the early 1990s by Louis Moresi [14][15]. It is a finite element that can solve convection problems within spherical coordinates. Although the code can solve different types or situations in convection using the properties of finite elements formalism, problems like temperature-dependent viscosity, pressure, position, composition, and stress-dependent viscosity are all possible to solve under this free software. The principal core for numerical modeling of any time-dependent convection situation is the solution of a motion and energy equation as we see on (3.1) taking into account the boundary conditions that involve the structurally and thermal differentiation in the planetary body.

When the initial conditions are imposed, then the momentum equation is solved, and we obtain the velocity that is used to address the advection-diffusion equation, giving as a result a new temperature. In that way, it is possible to run some script going back to the past to find the initial condition for a typical forward running initial and boundary value problem. This code uses an iterative solution scheme inside of this grid and also employs either a gradient solver or a full multi-grid solver to solve the discretized matrix equations.

For running the code, it is necessary to use MPI parallel programming, i.e., this procedure involves the use of several processors at the same time to reduce the running code time. In this case, it is necessary to divide all sphere into 12 "caps" or domains as we said in the last point, and each cap is going to be divided into other "sub-domains". The idea of creating this grid is to assign each domain to a different processor to make the calculations of vector velocities in heat terms in the three coordinates. In that way, the x-y direction will have three processors in execution, and the three remaining will be used to make the calculations in the respective nodes of the grid.

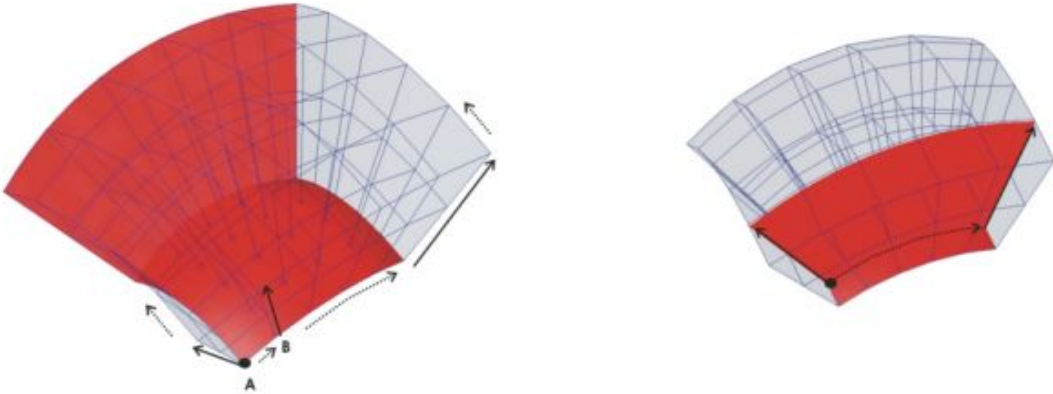


Figure 3.1: Scheme of multigrid for a full spherical problem [14][15].

3.4 Models Description

Initially, we seek to model the ice crust in Enceladus for two cases: in 2D and 3D. For the 2D model, it is planned to analyze the behavior of fluid mechanics in a sheet with 100 km thickness and with a temperature difference in the base and top. The description and full development of this model is found in Chapter 5.

On the other hand, in the 3D simulation, it is planned to do the same previous analysis but in spherical geometry, with the radius and intrinsic properties of the satellite [2] as input parameters.

In this research, we plan two types of simulations varying two parameters: Time and contrast viscosity [1]. We look for simulations with a fixed time and a fixed viscosity; we choose two intervals of time (4Ma-0Ma) and a uniform viscosity in the whole satellite. We produce other simulations with a fixed time again, and viscosity contrast of several orders of magnitude — all of this to study the plumes and heat time-evolution. In the next image, it is possible to see a scheme of the simulations routine that we are going to adopt in this case.

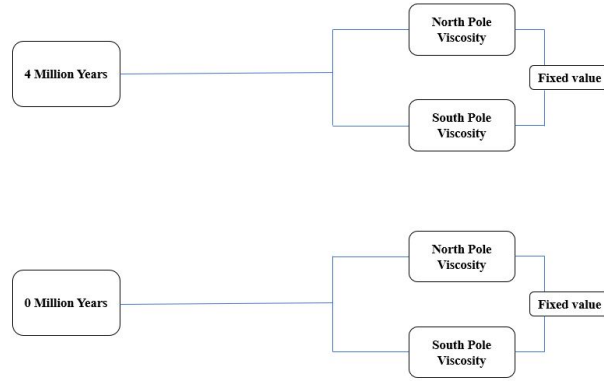


Figure 3.2: Simulation routine for the same viscosity contrast in all the crust.

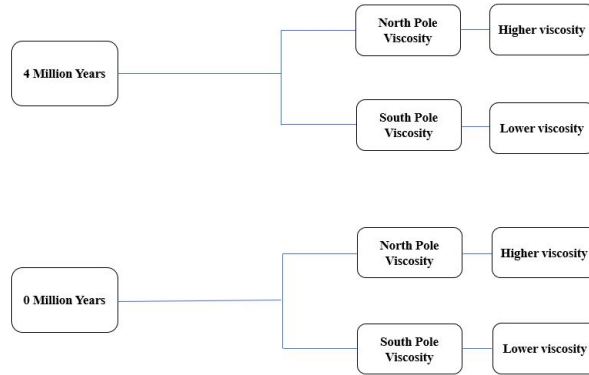


Figure 3.3: Simulation routine for a different viscosity contrast between north and south pole.

Chapter 4

Input files

4.1 Parameters

For running CitcomS, it is necessary to adopt Linux console, or in this case, we used the cluster console. The majority of data used as parameters of the program comes from the results obtained by Cassini in its first overflights on Enceladus [2]. Other settings are calculated, taking into account that the spherical shell to be simulated corresponds to a layer of ice that is not compositionally differentiated. Since only 1 % of this crust is constituted by Ammonia, Methane, among other elements, this ratio is not high enough to produce thermochemical convection [8][14]

Name	Command	Value
Crust thickness	thickness	100 km
Ice grain size	grainsize	0.3 mm
Gravity	gravity	0.114 ms^{-1}
Density	density	930 kgm^{-3}
Youngs modulus	young	1×10^{10}
Angular frequency	angularfreq	$2 \times 10^{-5} \text{ s}^{-1}$
Thermal expansivity	texp	$1.5 \times 10^{-4} \text{ K}^{-1}$
Thermal diffusivity	tdiff	$1.5 \times 10^{-6} \text{ m}^2 \text{ s}^{-1}$
Surface Temperature	surfacet	70K
Bottom Temperature	bottomt	273.15K
Specific Heat	specificch	$2150 \text{ JKg}^{-1} \text{ K}^{-1}$
Maximum compilation time	cpu-limits-in-seconds	360000000 s
Time Steps	minstep	200
Interval Between output files	storage-spacing	25
Rayleigh number	rayleigh	2.3×10^7
Maximum longitude	fi-max	1
Minimum longitude	fi-min	0
Nodes in X coordinate	nodex	17
Nodes in Y coordinate	nodey	17
Nodes in Z coordinate	nodez	9
Number of processors	nprocx	2
Number of processors	nprocz	2

Name	Command	Value
Minimum horizontal extent	theta-max	2.0708
Maximum horizontal extent	theta-min	1.0708
Perturbations Numbers	num-perturbations	1
Perturbation l	perturbl	1
Layers to be perturbed	perturblayer	5
Perturbation m	perturbm	1
Perturbation magnitude	perturbmag	0.05
Temperature dependency	TDEPV	on
Viscosity time-dependent	VISC-UPDATE	on
Maximum viscosity	VMAX	on
Minimum viscosity	VMIN	on
Number of material layers	num-mat=4	0.05
Output format	output_format	hdf5
The time-step interval between checkpoint output	checkpointFrequency	100
Disipation number	dissipation_number	0
Surface temperature	surfaceT	73
Gruneisen number	gruneisen	0
Internal Heating	Q0	5
Descontinuity depth	z_lith	100
Radius	radius	252e3
Density above	density_above	930
Density below	density_below	1500

Chapter 5

2D-Convection Model

5.1 Theory

The heat convection is a phenomenon well studied in dynamic systems. It describes a way in which heat is transferred through a fluid medium between surfaces or areas of a material with a different temperature. This phenomenon is also linked to other intrinsic processes of a body such as rotation, radiative transfer, phase changes, among others. When a portion of fluid raises its temperature, it expands, and its density decreases drastically. Knowing that this portion is in a gravitational field and heat is observed at the base of the sheet, it is assumed that the area above this hot parcel is a zone with lower temperature, as in the case of Enceladus. Therefore, this portion of fluid will tend to rise to the surface as long as the buoyancy overcome the resistance that has the viscosity and the term of thermal diffusion. In that case, it is necessary to introduce the Rayleigh Number and the Prandtl Number mentioned in the equations that governed this type of problem. Below is a brief description of each parameter:

5.1.1 Rayleigh number

This number describes a dimensionless quantity used in the study of fluid mechanics and is related to the way heat is transferred in a fluid medium. Below a critical value v_c , heat is transferred by conduction. On the other hand, when R_a is greater than v_c , heat transfer occurs by convection, as in this case [13]. Mathematically it is defined as:

$$R_a = \frac{g\rho\alpha\Delta TD^3}{\kappa\nu_0}$$

- g is gravity.
- ρ is density.
- α is thermal expansivity.
- ΔT is de temperature difference between the bottom and the surface.
- D is the depth of the system.
- κ is thermal diffusivity.
- ν_0 is the reference viscosity.

5.1.2 Prandtl number

The Prandtl number is a dimensionless quantity that relates the kinematic viscosity and the thermal diffusivity. In other words, it is proportional to the momentum diffusion and inversely proportional to κ . For convection situations, this quantity describes the thickness of the layers taking into account the thermal limit. It is defined as:

$$P_r = \frac{C_p \mu}{\kappa}$$

- C_p is the heat capacity at constant pressure.
- μ is the viscosity
- κ is the thermal conductivity.

5.1.3 Reynolds number

This amount defines the movement of a fluid, essentially at the group velocity level of the particles, depending on whether it is a laminar or turbulent flow. It relates the inertial and viscous forces found in a fluid (the latter come out from the Navier Stokes equation). Mathematically it is defined as:

$$R_e = \frac{\nu_s D}{\nu}$$



Figure 5.1: Convection patterns for Reynolds number $\sim 10^3$ [17].

5.2 Method

In this work, an initial model of the icy crust of Enceladus in 2D was proposed as an ice layer with different temperatures at the top and bottom. It was necessary to use two types of simultaneous solutions in a code Programming: Initially, a code implemented in python for cosmology problems was studied, especially Lattice-Boltzman simulations for collisional dark matter fluids (Acevedo, 2018). In this type of modeling, astrophysicists seek to study the behavior of "hot & cold" dark matter, taking into account that the temperature, in this case, refers to the kinetic energy of each zone of the deep universe, but this is a problem that is not going to be studied in this work.

What is essential about this logic of programming is that if the relativistic effects are ignored, the Lattice-Boltzmann equations approach in the classical limit to Navier-Stokes equations.

These mathematical relationships allow the study of the movement of Newtonian fluids; they can not be solved analytically, and therefore it is necessary to use numerical analysis to obtain an approximation of the respective solutions. For applying this model to the Enceladus ice shell problem, it required to change the boundary conditions and the initial conditions, which were obtained by previously analyzed data from the Cassini mission [2]. However, it was useful to merge this code with another code developed in Matlab to simulate the convection of heat in the atmosphere with a type of convection called Rayleigh-Benard, since it was necessary to construct convective cells that the cosmology code did not possess given the asymmetry which is found in the super galaxy clusters, but which is possible to see in the currents of the atmosphere [13]. This type of convection is simulated as a fluid layer with a temperature differential, where the upper and lower limits are rigid, waterproof, and isothermal, and the side walls are thermally insulated, as shown in the simulation for time = 0 (see Figure 5.1).

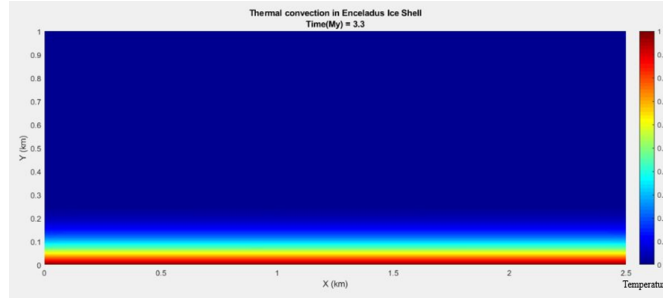


Figure 5.2: 2D convection model for an ice layer at $t=0$.

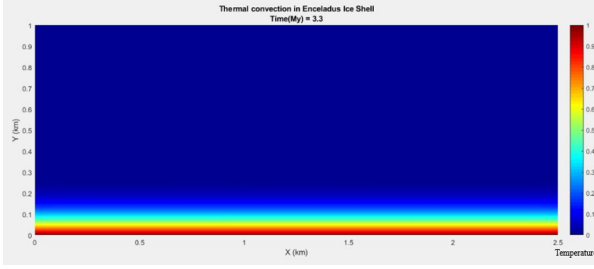
5.2.1 Time-evolution simulation

Taking into account the parameters mentioned above, a simulation was carried out in a laminar flow layer, which in this case was ice. Boundary conditions and analysis were assumed as:

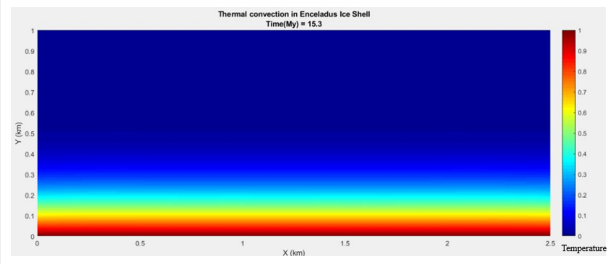
- Number of steps in $x=100$.
- Number of steps in $y=70$.
- Final time= 150 My.
- Width of time step= 0.01.
- Height of the layer=100 km.
- Length of the layer=70km.
- Top wall temperature=10 K.
- Bottom wall temperature= 273K.
- Reynolds number= 1500.
- Prandtl number= 7×10^7
- Rayleigh number= 2.3×10^7

5.3 Results

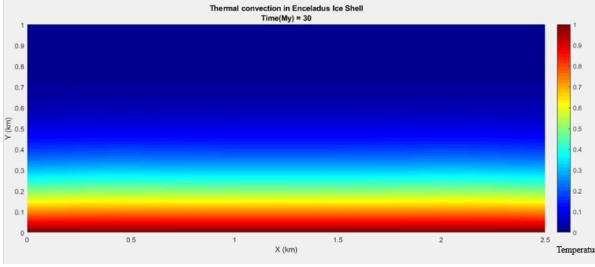
In this way, the simulation was performed in the course of 100 My. It is evident that for the first 40 My, no recognizable convection pattern is observed, and the velocity of diffusion is low. Starting at 50 My is possible to find the formation of two plumes that consequently reach the near-surface at 100 My, which would describe what is currently observed in Enceladus. For this simulation, no parallel components were used, since it is a 2D simulation did not require triangulating any mesh or nodes. The total time needed for the code was 8 minutes. A time-lapse of the simulation is shown below:



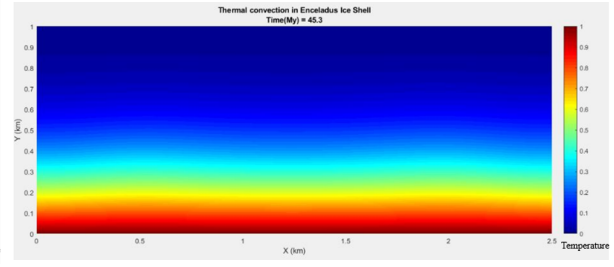
(a) Simulation of heat convection in an ice layer at $t = 0\text{My}$.



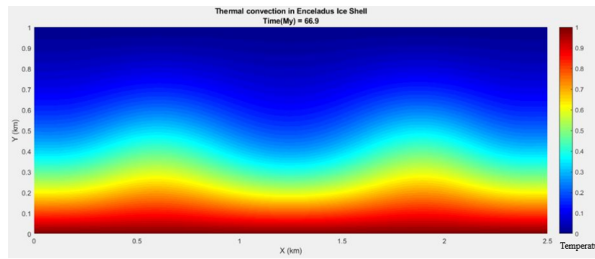
(b) Simulation of heat convection in an ice layer at $t = 15\text{My}$.



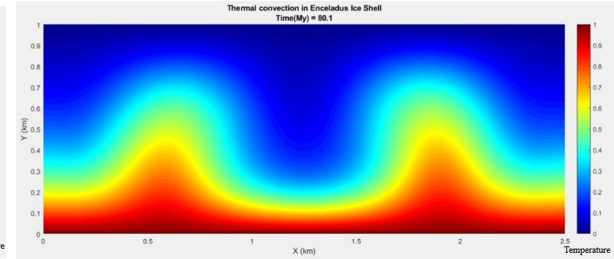
(c) Simulation of heat convection in an ice layer at $t = 30\text{My}$.



(d) Simulation of heat convection in an ice layer at $t = 45\text{My}$.



(e) Simulation of heat convection in an ice layer at $t = 60\text{My}$.



(f) Simulation of heat convection in an ice layer at $t = 75\text{My}$.

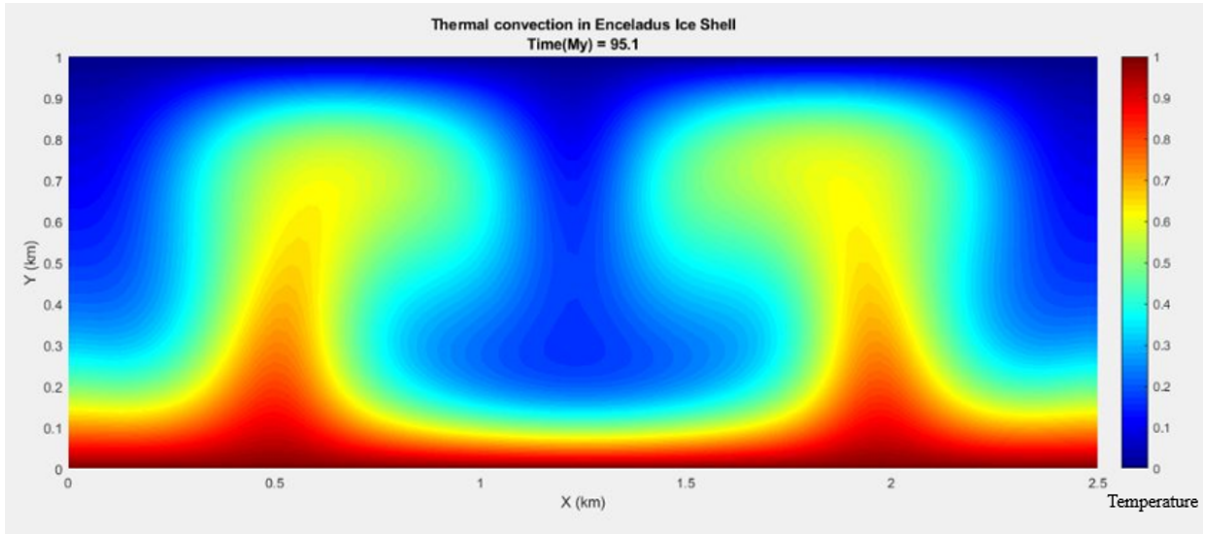


Figure 5.4: Simulation of heat convection in an ice layer at $t = 100\text{My}$.

Figure 5.5: All the graphs shown above were developed with Matlab after merging the cosmological simulation code (Acevedo, 2018) and the Rayleigh-Benard convection code [14]. The temperature scale is normalized, it means that each value is divided by 273K, by suggestion of [1], for simplicity in the handling of the data. In this way, it is observed that the first 50 My plumes do not develop enough to reach the surface and grow slowly. However, starting at 51 My, it begins to see the growth and float of these plumes to an area close to the surface. If we analyze the horizontal distance that separates each convection pattern, we find a length equivalent to 150 km, a value very close to that found in the “Tiger Stripes” [2].

Chapter 6

3D-Convection Model

6.1 Method

In this chapter, the development of 3D modeling of the Enceladus icy crust will be studied. As already mentioned, this procedure was performed through free software CitcomS. Initially, it was established to divide the spherical shell into several elements, since the method to be implemented by the software was to be precisely finite elements. Below is a 3D figure of how the surface of Enceladus would fragment.

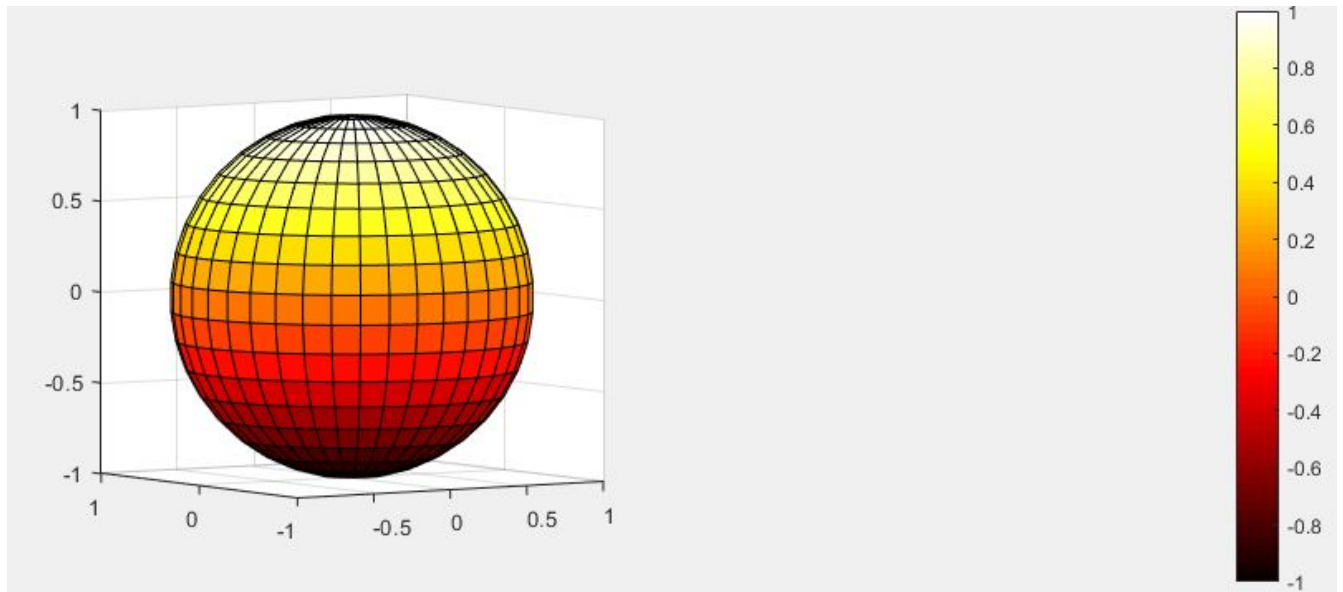


Figure 6.1: 3D scheme of the fragmentation of the entire crust in finite elements.

6.1.1 Running simulations in the cluster

The idea is to assign to each intersection of the grid shown above a corresponding node or point, for which the viscosity, temperature, and velocity are calculated. To solve partial differential equations in this multidimensional grid, it was necessary to resort to the resources of the cluster that belongs to the Universidad de los Andes. This was done to reduce the times during which the simulation

was run. If a single processor had been used, the elapsed time would have reached three days for each attempt. Being a 6-month investigation, it was necessary to optimize the simulation time. The distribution of nodes and finite elements in the southern hemisphere of the study satellite is shown below.

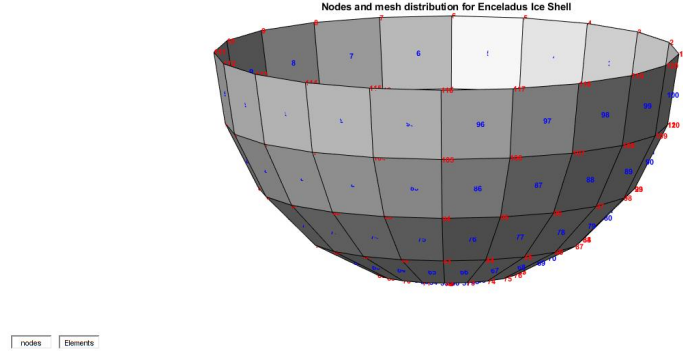


Figure 6.2: Nodes and mesh distribution in Enceladus South Pole.

6.1.2 MPI computing

Parallel computing consists of executing several simultaneous tasks in different processors. In this case, the sphere was divided into 12 equal pieces, and each piece was assigned a single processor. During the executing of the task from the cluster console, the numerical calculation for each point in the mesh will begin simultaneously. In this way, there will be a connection between the data, which will allow the triangulation of the coordinates, and later, when plotting, it will enable showing the information of all the characteristics at the same time. i.e., For the corresponding finite element, the velocity, viscosity, and temperature variables are plotted. It is essential to highlight that 12 processors were assumed by the structure that follows the cluster of the Universidad de los Andes, which follows behavior in powers of 4. For that reason, the input file was told to use 16 processors, but we only did the calculations in 12. The following figure shows the corresponding grid assigned to each terminal

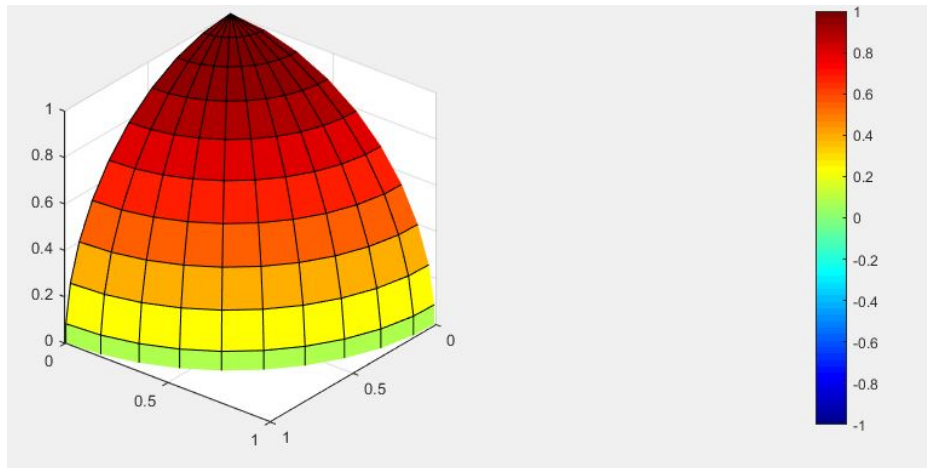


Figure 6.3: Multidimensional mesh for uni-processor.

6.1.3 HDF5 files

CitcomS allows output files with extension hdf5, ASCII, or VTK. The last two require additional processing because, for each time-step, they generate a txt file, and this is repeated for each processor. This situation can be quite challenging to interpret since, for this case, there are 12 processors and 1000 time-steps that generated 5700 .txt files approximately, which took a large amount of memory and required to be combined for each time-step separately. This procedure was not efficient, taking into account that there were parameters that did not have the same time-step size, so finally, we chose to use the .hdf5 files.

The Hierarchical Data Format (HDF) is a format extension developed at the National Center for Supercomputing Applications (NCSA). It is designed for storing, retrieving, analyzing, visualizing, and converting scientific data, especially multidimensional arrays [15][16]. As the name implies, it uses a hierarchical structure composed of groups that contain inner-subgroups of datasets. In this way, each output file that was obtained came in the following structure:

- Enceladus.0.h5

That contains in its interior the information related to all 12 processors in time-step 0.

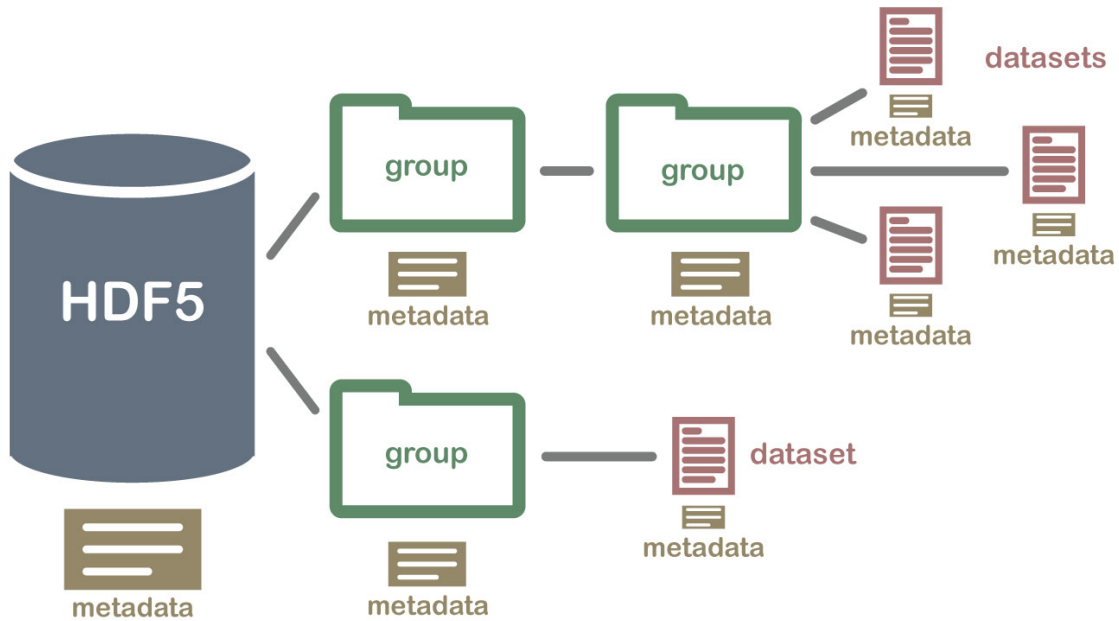


Figure 6.4: Hierarchical Data format structure, taken from: National Ecological Observatory Network (NEON).

6.2 Results

Several simulation attempts were made to maintain a reasonable number in the calculation of flux energy on the surface of the south pole of Enceladus. Therefore, it was simulated for three different times (0 My, 50 My, 100 My), to find some correlation with the results obtained in the 2D model exposed in the previous chapter.

6.2.1 0 Million years

For this simulation, to adopt small tide dissipation does not allow the existence of an ocean below the surface. For this case, we have an isothermal surface (200K) trying to simulate Enceladus shortly after its formation. Authors as [4] attribute the observed heat as a result of a meteorite impact that led Enceladus to change its orbit and its eccentricity, this simulation would be throwing the convective appearance of Enceladus at a time before the eccentricity change. Then, the crust is estimated with a uniform viscosity contrast in both hemispheres, so it is evident that no detectable convection patterns are observed neither in the mesh nor in the respective poles.

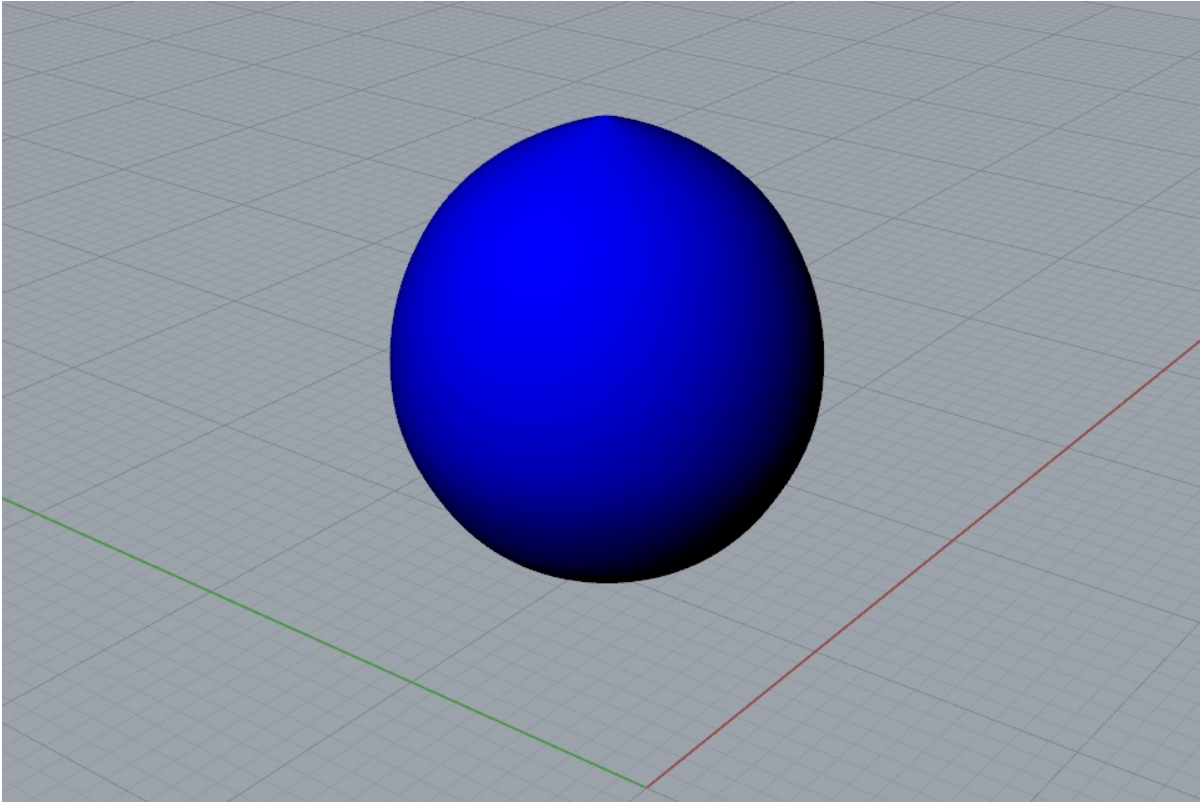


Figure 6.5: Simulation of heat convection in an ice layer at $t = 0\text{My}$.

6.2.2 50 Million years

In this situation, Enceladus was simulated with an elapsed time of 50 My, following the assignment of parameters as in [1]. A specific array was used to separate the surface layer of the northern

hemisphere in the respective spherical coordinates and terms of the corresponding nodes and processors. These, to simulate the convection under a non-convective layer, which would explain the tectonic inactivity in the northern hemisphere. However, the .hdf5 extension data was plotted with the information contained in velocity and temperature.

When entering the parameters, many items were related to convective problems in the Earth's mantle, because the documentation of CitcomS did not have clear information about the arguments that they received. For this reason, the appearance of two rising plumes in both poles is evidenced. In agreement with [1], these plumes appear when the viscosity contrast is the same for the north and south zone, and the Rayleigh number has a value of 6.5×10^7 . However, the convection patterns that are observed are quite irregular, but they differentiate the latitudes of the south pole. This model is more accurate than the previous one, even though the calculation of energy flow yielded a figure of several orders of magnitude higher than the value observed by the Cassini mission ($\sim 10\text{GW}$) [7].

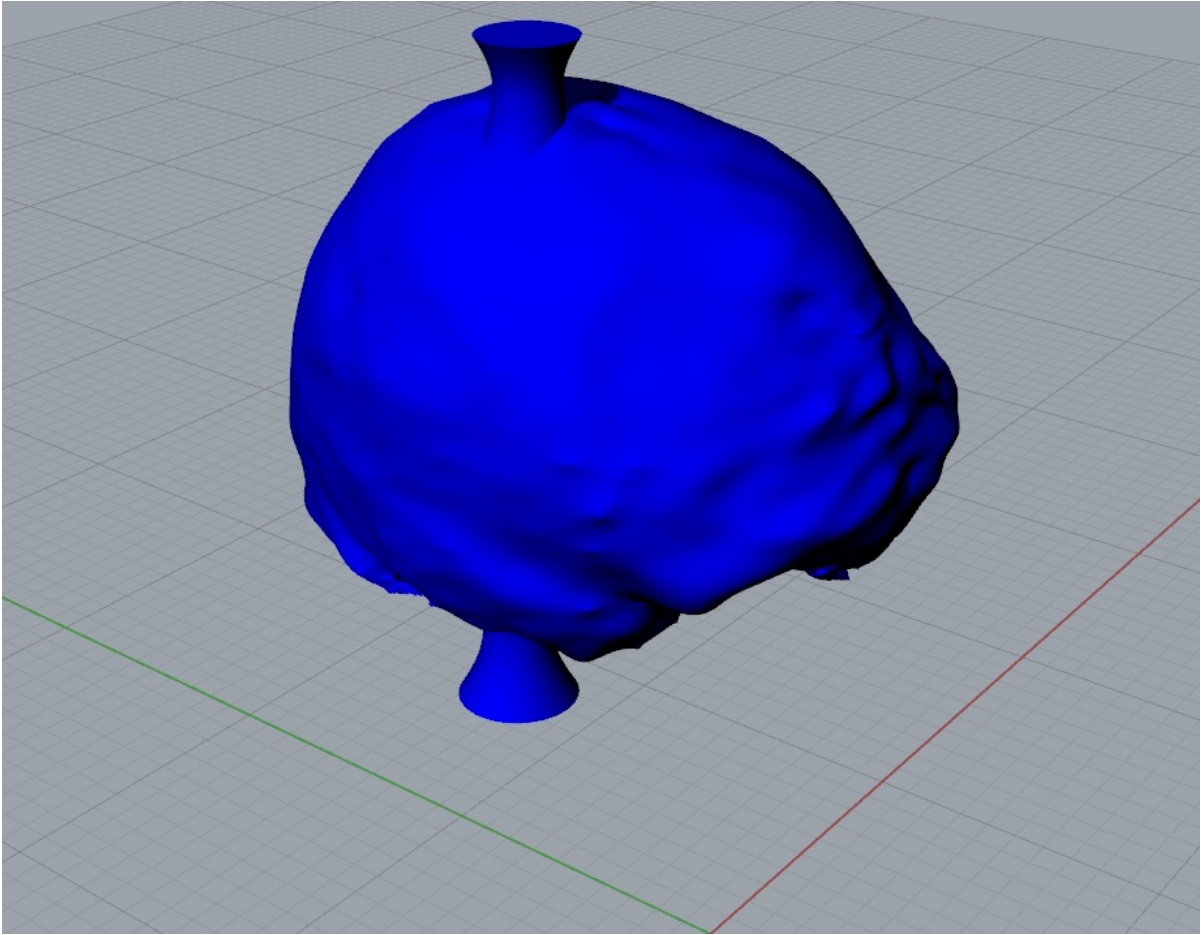


Figure 6.6: Simulation of heat convection in an ice layer at $t = 50\text{My}$.

6.2.3 100 My

Finally, for this simulation was taken into account that the viscosity is temperature-dependent; this relationship is inversely proportional so that a high temperature will lead to low viscosity and vice-versa. In this way, a viscosity of 1×10^3 was set at the south pole and a viscosity of 1×10^5 for

the north pole. The Rayleigh number is maintained as in Chapter 4, following [1], it is provided that the zone that will cover the low viscosity will be below 60 S latitude. To understand the data sets contained in each file, it was possible to see graphically the structure in which each one was and then graph separately for each processor. These were achieved through the executable package of HDFView, which is available to the scientific community working with Big Data. Also, this package contains the HDFExplorer tool that allows you to visualize and graph. In this case, the appearance of a single feather in the southern hemisphere is observed, as shown in Figure 6.7:

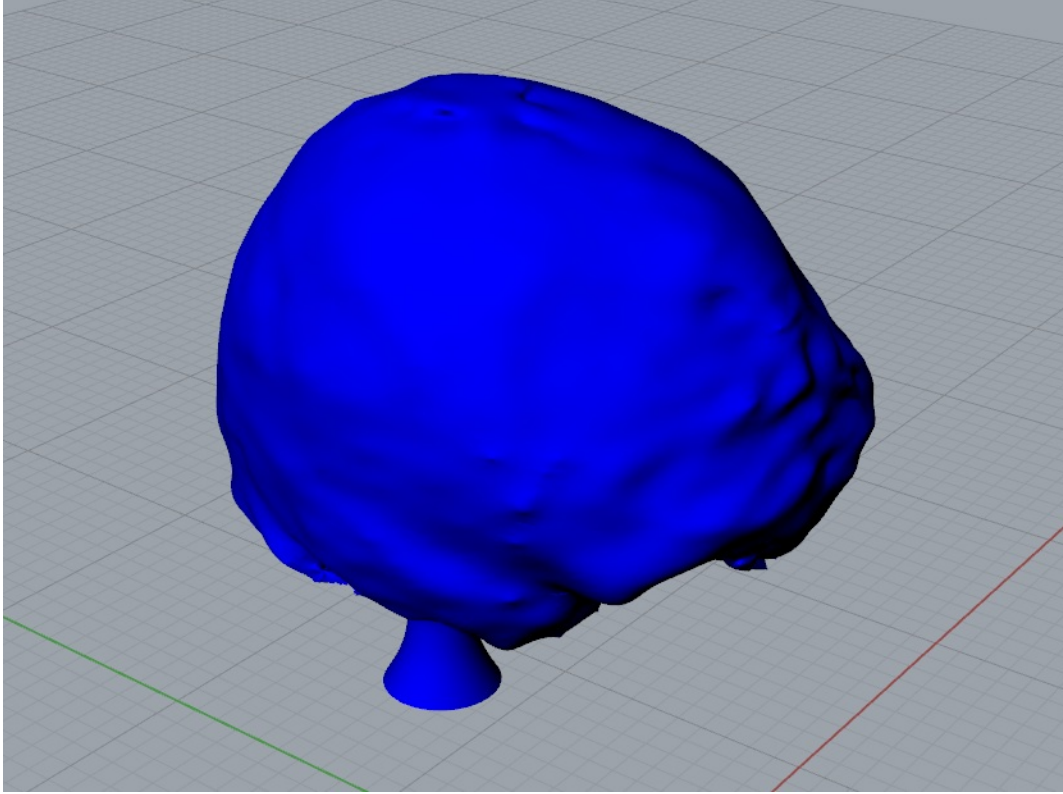


Figure 6.7: Simulation of heat convection in an ice layer at $t = 100\text{My}$. The plot shows the temperature structure for a 3D model with a single plume at the south pole, some irregularities are shown at the Equator as a result of the Earth mantle's convection input parameters imposed by default by CitcomS.

Energy results

All these simulations were calculated in approximately 5 hours each. It was not possible to graph the results with the viewers recommended by the CitcomS development team. These viewers were OpenDX and Mayavi2, which could read .h5 files with the help of some packages offered by a host that was not part of the developers. During the download of the packages from the Unix console, the remote connection to that server could not be generated. For this reason, it was not possible to download and display the data under that 3D scientific data visualization environment.

In this case, the value obtained at the end of the simulation for the surface heat flow was 9.6 GW. This value is much higher than observed by Cassini (10 GW approximately) [2]. The final numerical result of the last simulation is shown below:


```
(999) 16.0 s v=2.207415e+03 p=4.375706e+05 div/v=3.66e-04 dv/v=2.75e-06 dp/p=1.22e-06 step 1000
(1000) 16.0 s v=2.207415e+03 p=4.375703e+05 div/v=3.62e-04 dv/v=2.69e-06 dp/p=1.20e-06 step 1000
Angular momentum: rot=3.624994e+02 tr=9.475559e+01 fr=8.652810e+01
surface heat flux= 9.610444
bottom heat flux= 23.450922
cycles=1000
Average cpu time taken for velocity step = 8.346547
```

Figure 6.8: Numeric results from Cluster console.

Chapter 7

Conclusions

Simulations in 2D and 3D allowed concluding: In the 2D model, there is evidence of great heat storage during the first 50 million years with a subsequent release of energy in the form of plumes that reach the nearby surface. These plumes show the convection patterns that were expected to be found, being consistent with the “Tiger Stripes” heat pattern observed in 2005 by Cassini. Even so, the 2D model was only an approximation to an ideal layer of ice. Many relevant factors were omitted, such as the presence of chemical elements, the topography in the south pole of Enceladus (which manages to rise several meters in altitude) [2] as a consequence that it can affect the angular momentum that Enceladus has and its effect on the tidal forces. On the other hand, the results of the renewal of the surface by the particles that fall back due to gravity were not taken into account, and that is possibly the reason why there is little or no evidence of the number of craters in the south pole. For two dimensions, the mechanical properties of the ice were also omitted and the limits that can be had under those conditions, i.e. Fracture criteria, ice relaxation, deformation, among others.

On the other hand, the 3D simulations were more complete, since they included the attributes that the previous model did not have. CitcomS calculated the velocity, viscosity, and temperature for each point of the sphere as assigned in the grid to each processor. Therefore, it was necessary to use the parallelization, to be able to differentiate the coordinates of the pole in which the viscosity value was lower due to the temperature dependence. At 50 My, this model has a limitation because it shows the presence of two plumes in both poles, and it is precisely not what is observed, or there is evidence that it has happened in Enceladus. This can be explained, in the course of the simulation, the viscosity contrast between the north and south poles was varied, and at 50My, there was an intersection in this variation and both polar areas reached to have the same viscosity contrast, under the same conditions that is why two plumes appear the same but in opposite directions.

At 100 My, the presence of a plume in the south pole is observed, with a surface energy flow of 9.6 GW, which suggests in the numerical results that the base of the ice sheet must have 23.4 GW of heat flux. This, combined with the irregularity that was obtained in the spherical symmetry, could be explained as the result of combining default parameters in the input file. Since CitcomS is written in a configuration that simulates the Earth’s mantle, the instructions in the manual are guided to those parameters without the user’s permission. In this way, irregularities are observed in the 3D plot towards the equatorial zones.

It is important to emphasize that both models converge at an initial point without heat flow at 0 My and a subsequent release of heat at 100My, which would be the current time at Enceladus.

This allowed us to study the temporal evolution of plumes and establish that initially, Enceladus stored a large amount of energy, and convection began its development halfway through time. In this way, a type of episodic thermal convection can be established with maximum heat peaks, as suggested in [3].

It is possible to analyze that by varying the Rayleigh number, the model can change drastically. Taking into account that, for values $j \cdot 10^3$ convection heat transfer occurs. If that value were lowered, it could be argued that mechanically the south pole could become weaker than the northern polar areas [1]. The parameters that were entered as input file can be changed to obtain more accurate results, such as latitudes that reach the south pole with a different temperature because according to [3] the displacement and deformation of the ice crust reach 0.5 m / year, which in geological scales can change the latitudes of the weak south pole.

Finally, the same conclusion that all the authors investigating Enceladus have is highlighted: It is not possible to know how the heat was generated in Enceladus, taking into account that neither the tidal forces, nor the radiogenic heat, nor the shear friction reaches cause such high energy values as those observed by Cassini in 2005. Also, this observational value is changing in the way that a more excellent range of wavelengths is covered in remote sensor observations. Therefore, the origin of this phenomenon is still a matter of investigation for future work.

Bibliography

- [1] Han, L., Tobie, G., Showman, A. P. (2012). The impact of a weak south pole on thermal convection in Enceladus' ice shell. *Icarus*, 218(1), 320-330.
- [2] Porco, C. C., Helfenstein, P., Thomas, P. C., Ingersoll, A. P., Wisdom, J., West, R., ... Kieffer, S. (2006). Cassini observes the active south pole of Enceladus. *science*, 311(5766), 1393-1401.
- [3] Nimmo, F., Spencer, J. R., Pappalardo, R. T., Mullen, M. E. (2007). Shear heating as the origin of the plumes and heat flux on Enceladus. *Nature*, 447(7142), 289.
- [4] Meyer, J., Wisdom, J. (2007). Tidal heating in Enceladus. *Icarus*, 188(2), 535-539.
- [5] Hana, L., Tobieb, G., Showmanc, A. P. (2011, March). The Dichotomy of Thermal Convection in Enceladus' Ice Shell. In *Lunar and Planetary Science Conference* (Vol. 42, p. 2211).
- [6] Barr, A. C. (2008). Mobile lid convection beneath Enceladus' south polar terrain. *Journal of Geophysical Research: Planets*, 113(E7)
- [7] Běhounková, M., Tobie, G., Choblet, G., Čadek, O. (2010). Coupling mantle convection and tidal dissipation: Applications to Enceladus and Earth-like planets. *Journal of Geophysical Research: Planets*, 115(E9).
- [8] Brown, R. H., Clark, R. N., Buratti, B. J., Cruikshank, D. P., Barnes, J. W., Mastrapa, R. M., ... Bellucci, G. (2006). Composition and physical properties of Enceladus' surface. *Science*, 311(5766), 1425-1428.
- [9] Durham, W. B., Stern, L. A. (2001). Rheological properties of water ice—Applications to satellites of the outer planets. *Annual Review of Earth and Planetary Sciences*, 29(1), 295-330.
- [10] Goldsby, D. L., Kohlstedt, D. L. (2001). Superplastic deformation of ice: Experimental observations. *Journal of Geophysical Research: Solid Earth*, 106(B6), 11017-11030.
- [11] Grott, M., Sohl, F., Hussmann, H. (2007). Degree-one convection and the origin of Enceladus' dichotomy. *Icarus*, 191(1), 203-210.
- [12] Han, L., Showman, A. P. (2005). Thermo-compositional convection in Europa's icy shell with salinity. *Geophysical research letters*, 32(20).
- [13] Chillà, F., Schumacher, J. (2012). New perspectives in turbulent Rayleigh-Bénard convection. *The European Physical Journal E*, 35(7), 58.
- [14] Ismail-Zadeh, A., Tackley, P. (2010). *Computational methods for geodynamics*. Cambridge University Press.

- [15] Zhong, S., M.T. Zuber, L.N. Moresi, and M. Gurnis (2000), The role of temperature-dependent viscosity and surface plates in spherical shell models of mantle convection. *J. Geophys. Res.*, 105, 11,063-11,082
- [16] Tan, E., E. Choi, P. Thoutireddy, M. Gurnis, and M. Aivazis (2006), GeoFramework: Coupling multiple models of mantle convection within a computational framework, *Geochem., Geophys., Geosyst.* 7, Q06001, doi:10.1029/2005GC001155
- [17] Tansley, C. E., Marshall, D. P. (2001). Flow past a cylinder on a plane, with application to Gulf Stream separation and the Antarctic Circumpolar Current. *Journal of Physical Oceanography*, 31(11), 3274-3283.
- [18] Acevedo Barroso, Javier (2018). Simulating collisional dark matter using a Lattice Boltzmann method. (Monografía de pregrado). Universidad de los Andes, Bogota-Colombia. <https://github.com/ClarkGuilty/CollisionalDarkMatterSimulation>
- [19] Thompson, C. M., Shure, L. (1995). Image Processing Toolbox: For Use with MATLAB;[user's Guide]. MathWorks.
- [20] Suraj Shankar(2012). Thermal gradient driven natural convection is simulated in a 2D domain. Obtained from: https://la.mathworks.com/matlabcentral/fileexchange/38093-rayleigh-benard-convection?s_tid=prof_contriblnk
- [21] Neukum, G. (1985). Cratering records of the satellites of Jupiter and Saturn. *Advances in Space Research*, 5(8), 107-116.